

A YOUNG RADIO-EMITTING MAGNETIC B STAR IN THE RHO OPHIUCHI CLOUD

PHILIPPE ANDRÉ

Institut de Radio Astronomie Millimétrique, Granada, Spain

THIERRY MONTMERLE

Service d'Astrophysique, Centre d'Etudes Nucléaires de Saclay, Gif-sur-Yvette, France

ERIC D. FEIGELSON AND PETER C. STINE

Department of Astronomy, The Pennsylvania State University

AND

KARL-LUDWIG KLEIN

Observatoire de Paris, Section de Meudon, France

Received 1987 November 3; accepted 1988 June 15

ABSTRACT

As part of a Very Large Array study of the continuum radio sources associated with the ρ Oph molecular cloud, we report the first detection of circular polarization from a young stellar object, the luminous infrared source S1. This object coincides with an embedded B star having an unusually high X-ray luminosity. The presence of a weak, compact H II region confirms the early type and suggests a very young star. The circularly polarized radio emission cannot come from a thermal plasma because this would imply an unrealistically high magnetic field. Interpretations in terms of flares, which are usually invoked to explain nonthermal emission from active stars, is unlikely because of the nonvariability of the radio source. Optically thin gyrosynchrotron radiation from energetic electrons in the outer parts of a magnetosphere similar to that of chemically peculiar magnetic stars provides a better model. Such a magnetosphere also features a coronal region which would explain the X-ray emission as well. S1 may thus be the youngest magnetic B star ever reported. If this interpretation is correct, our observations of S1 shed a new light on the mechanism responsible for the radio emission from Bp–Ap stars recently discovered by Drake and coworkers.

Subject headings: stars: magnetic — stars: pre-main sequence — stars: radio radiation — stars: X-rays

I. INTRODUCTION

Recent observations have shown that young stellar objects (YSOs) can be detected at various wavelengths from radio to X-rays, giving insight into various stages of pre-main-sequence (PMS) stellar evolution. The X-ray domain has proved a powerful tool for detecting moderately embedded ($A_v < 10$) YSOs over areas covering up to several square degrees, sometimes outnumbering the classical T Tauri stars (TTs) by a factor of more than 2 or 3 (e.g., Feigelson 1984, 1987). In a given star-forming region, such as the ρ Ophiuchi cloud (160 pc away from the Sun), X-ray sources are found among all stellar types, from early B to mid-M, with the dominant X-ray emission coming from bremsstrahlung associated with giant flares (Montmerle *et al.* 1983, hereafter MKFG).

It is a logical next step to perform sensitive radio observations of such star-forming regions, looking for nonthermal emission (e.g., flares from X-ray sources) as well as thermal emission (e.g., ionized winds from TTs or compact H II regions associated with early-type stars). André, Montmerle, and Feigelson (1987, hereafter AMF) have recently undertaken a survey of the ρ Oph cloud region with the Very Large Array, over several square degrees at various frequencies and configurations. Whereas the X-ray detection rate of YSOs is high, with 40–60 sources in the cloud, AMF find a small radio detection rate with 8–13 stellar sources down to the ~ 1 mJy level. The radio detection rate of classical TTs is also low. Of special importance is a highly variable stellar radio emission from DoAr 21, a non-TT K–G PMS star, which was interpreted as the first evidence for a radio flaring YSO (Feigelson and Montmerle 1985).

A more extensive study (Stine *et al.* 1988; André *et al.* 1988) has revealed several other radio YSOs. The purpose of the present paper is to single out an unusual radio source associated with an embedded X-ray-emitting visible star, first identified as the counterpart to the brightest near-IR source of the ρ Oph cloud by Grasdalen, Strom, and Strom (1973), and referred to as S1. This object has been already observed in the GHz range by Brown and Zuckerman (1975), Falgarone and Gilmore (1981), and AMF. But the novel features present in our recent data point to a YSO having a unique, complex radio structure, consisting in a nonthermal unresolved core surrounded by a thermal extended halo. Section II presents the radio observations of S1, and in particular reports the first detection of circular polarization from a young radio star, while § III summarizes the properties of this object at other wavelengths. We interpret the radio emission of the halo in § IV. We discuss the core in § V and present a quantitative model in § VI. Our main conclusions are summarized in § VII.

II. RADIO OBSERVATIONS AND RESULTS

a) Observations and Data Reduction

Long-exposure observations of S1 were obtained in 1987 February when the VLA was in its C/D hybrid configuration. Approximately 2 hr of on-source integration at 15 GHz on February 13, and 2.5 hr at 5 GHz on February 15, were used to make maps. Antenna phases and gains were adjusted to the nearby calibrator 1622–297, whose flux was bootstrapped to 3C 286. Scans of S1, alternating with runs on the calibrator, were homogeneously spread over 3 hr on February 13 and 5 hr on February 15 to maximize the u - v coverage. Standard VLA

bands with 100 MHz total bandwidth were used. Observing conditions were good except for antenna shadowing during the first ~ 1.5 hr of the February 15 run, due to the compact configuration and southern declination of the source. Fourier-transformed maps in the four Stokes parameters were made and CLEANed using the task MX in NRAO's Astronomical Image Processing Systems (AIPS) on concatenated A/C and B/D data bases. In making these maps, we used natural weighting to get the maximum sensitivity to weak sources and faint extended emission, although this choice results in a synthesized beam 20%–50% broader than with uniform weighting of the visibility data. The 5 GHz intensity map, made of 512×512 pixels, covers a $18'.8$ square and was CLEANed to remove the sidelobes of nearby contaminating sources. The size of the synthesized beam is $\sim 17'' \times 17''$ (FWHM), and the rms deviation, measured in source-free portions of the map, is 0.036 mJy beam $^{-1}$. Since S1 appeared extended, the integrated flux density was estimated by summing pixel values within boxes, on the one hand, and by using the visibility curve, on the other hand. The errors in the flux densities reported below include only the statistical noise; an additional uncertainty of up to 3% due to calibration may be present. At 15 GHz, we only made a 256×256 pixel CLEANed map covering a $3'.2$ square, because a larger, dirty map revealed no confusion sources. The beam size is $4'.5 \times 3'.8$, and the rms is 0.079 mJy beam $^{-1}$.

b) Morphology of the Radio Source

In our 5 GHz map (Fig. 1a), the central radio source coincides with the near-infrared source S1 (optical star on the Palomar Sky Survey Red Print) to within $2''$. From 1985 15 GHz observations with a higher resolution (see below), the position of the radio peak is known to better than $0'.1$: $\alpha = 16^{\text{h}}23^{\text{m}}32^{\text{s}}.74$ and $\delta = -24^{\circ}16'44''.3$. The source consists of a strong (~ 8 mJy; see below) unresolved core surrounded by a

faint halo (~ 4 mJy distributed over $\sim 20''$) which seems to extend toward the northeast (p.a. $\sim 45^{\circ}$). Approximately $40''$ southeast lies a weak source [flux densities 0.95 ± 0.05 mJy at 5 GHz, 0.45 ± 0.08 mJy at 15 GHz, hence a spectral index $\alpha(5, 15) = -0.7 \pm 0.2$] that looks like a companion of S1 on Figure 1a. Observations using the A array made on 1987 August 6 have revealed that it is a point source, located at $\alpha = 16^{\text{h}}23^{\text{m}}32^{\text{s}}.87$, $\delta = -24^{\circ}17'21''.8$.

Because Gaussian fitting failed in the image plane, we modeled the core-halo structure directly in the u - v plane. The Fourier transform of the CLEANed components corresponding to the strong (map flux density ~ 14 mJy) contaminating source BZ 6 (Oph 6 of Brown and Zuckerman 1975; ~ 6.7 away from S1) was first subtracted from the u - v data base using the AIPS task UVSUB. After this removal, the only source that somewhat hinders the analysis is the weak "companion." Its contribution to the visibility curve was estimated, and error bars on the visibility points were correspondingly increased on the shortest baselines (sensitive to a $\sim 40''$ extent). The phase center was shifted to the map peak position of S1. Following the procedure first used by White and Becker (1982; see also Seaquist and Taylor 1987), the u - v plane was then divided into annular rings, and the real components of the visibilities were averaged azimuthally in each ring (the imaginary parts are of no interest in such an average which removes departures from circular symmetry, because the visibilities of a circularly symmetric source are real). Figure 2a shows the resulting vector-averaged visibilities plotted against projected baseline lengths. This observed visibility curve was compared with a two-component model corresponding to a point source surrounded by a circularly symmetric Gaussian halo. A detailed least-squares fit to the data was not made because such a simple model is not intended to represent the actual intensity distribution of the halo but only to give estimates (furthermore, the

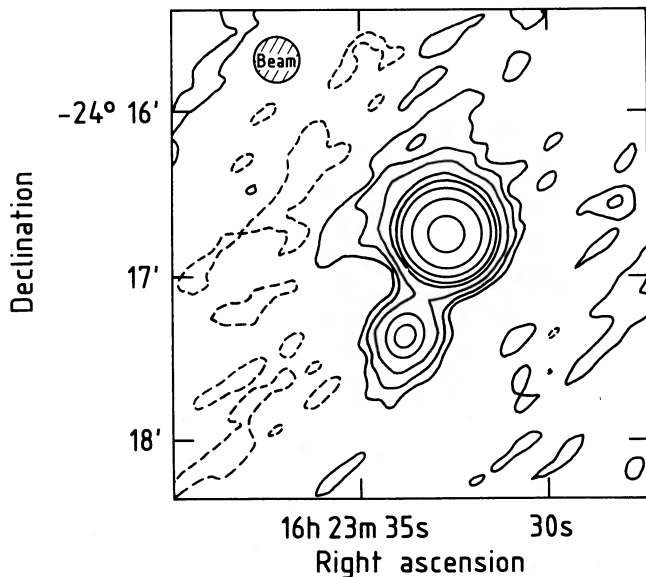


FIG. 1a

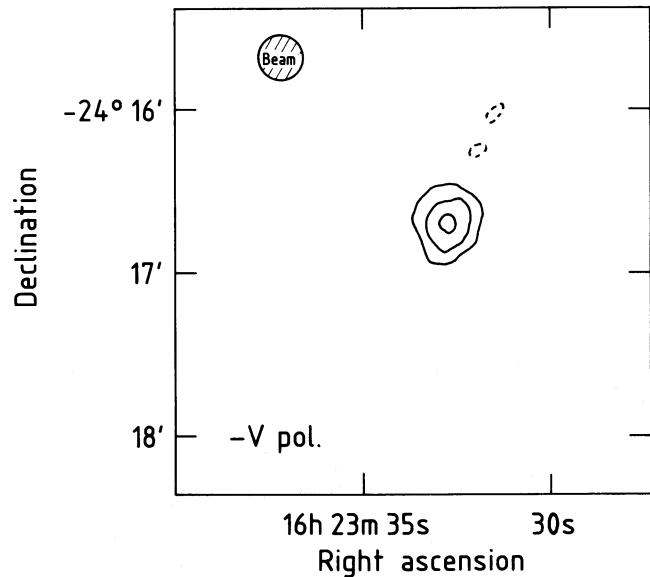


FIG. 1b

FIG. 1.—(a) Partial VLA 5 GHz map (C/D configuration) centered on S1. The main radio source is surrounded by a diffuse halo. The apparent connection to the secondary radio sources, $\sim 40''$ to the southeast, is not necessarily real. The contour levels are 60%, 40%, 15%, 7.5%, 4.5%, 3%, 1.5%, 0.75%, 0.4%, and -0.4% of the peak flux density 10.24 mJy beam $^{-1}$. This peak flux overestimates the flux density of the core (see text). The FWHM synthesized beam is indicated at the upper left. (b) Same as (a), in the Stokes parameter V (circular polarization). The contour levels are 18%, 44%, and 88% of the negative peak flux density of -0.57 mJy beam $^{-1}$. There is no background contour higher than -18% of the peak flux. The source appears unresolved and is consistent with being associated with the S1 core (see text).

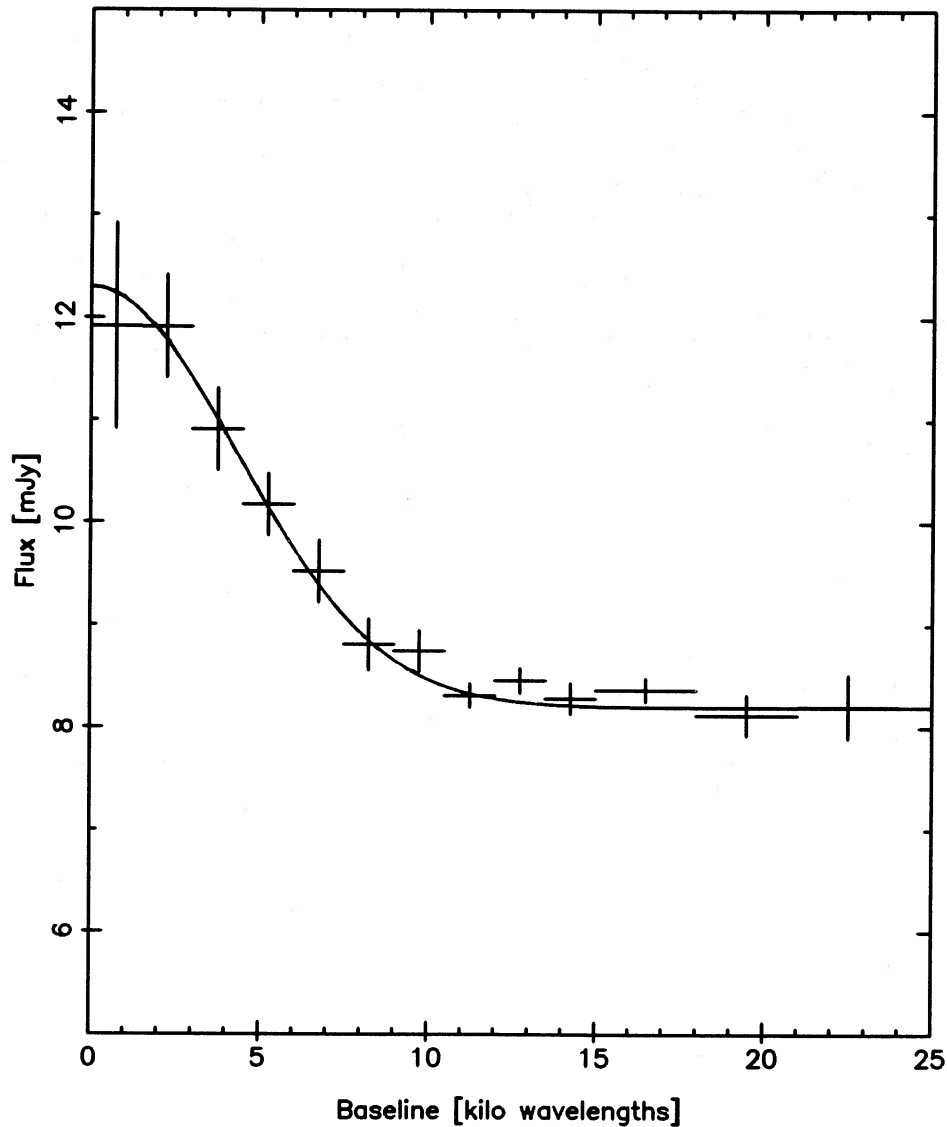


FIG. 2a

FIG. 2.—(a) Vector-averaged visibility function of S1 at $\lambda = 6$ cm. Vertical lines represent error bars for observed visibilities, and horizontal lines are the ranges of baselines included in the average. The solid line shows the visibility curve of a two-component model consisting of an 8.2 mJy point source and a circular Gaussian distribution with a 4.1 mJy total flux and a $9''$ half-power radius. (b) Same as (a), but for $\lambda = 2$ cm. The core is represented by an 8.0 mJy point source, and the halo by a Gaussian distribution with a 3.7 mJy total flux and an $11''.5$ half-power radius. In both cases (6 and 2 cm), a few bins corresponding to the largest baselines are omitted because they are undersampled and hence have very large error bars.

noise introduced by the “companion” is non-Gaussian). Nevertheless, this analysis yields the ranges of parameters which give reasonable fits: 8.2 ± 0.3 and 4.1 ± 0.7 mJy for the 5 GHz flux densities of the core and the halo, respectively, and $9'' \pm 2''$ for the half-power angular radius of the halo. While these parameters are only indicative for the halo because of missing short baselines, we have confidence in the flux density of the core, which is accurately determined by the plateau seen on the visibility curve for baselines greater than 10 k λ . Adding the flux densities of the two components gives a total flux density of 12.3 mJy (± 0.6 mJy from the visibility analysis), which matches the 12.1 mJy (± 0.1 mJy from the statistical noise of the map) found by integrating all the map pixel values within a $\sim 45'' \times 45''$ box centered on S1.

The core-halo structure is also present at 15 GHz, and we performed a similar visibility analysis at this frequency (Fig.

2b). This was somewhat easier because of the absence of strong contaminating sources and because of the lower flux density of the “companion” at 15 GHz. We estimate the 15 GHz flux densities to be 8.0 ± 0.3 and 3.7 ± 0.8 mJy for the core and the halo, respectively, and the half-power angular radius of the halo to be $11''.5 \pm 3''.5$. The sizes of the halo are thus identical (within the error bars) at 5 and 15 GHz.

c) Polarization Data and the Puzzle of the S1 Radio Core

A new and fundamental result of the present study is the detection of circular polarization from S1. At 5 and 15 GHz, our maps in the Stokes parameter V have rms of 0.03 and 0.08 mJy, respectively, and we find $V_{5 \text{ GHz}} = -0.57$ mJy ($19 \times$ rms detection) and $V_{15 \text{ GHz}} = -0.57$ mJy ($7 \times$ rms detection). (A negative Stokes parameter V corresponds to a left-handed circular polarization; see Bignell 1982.) Figure 1b illustrates the

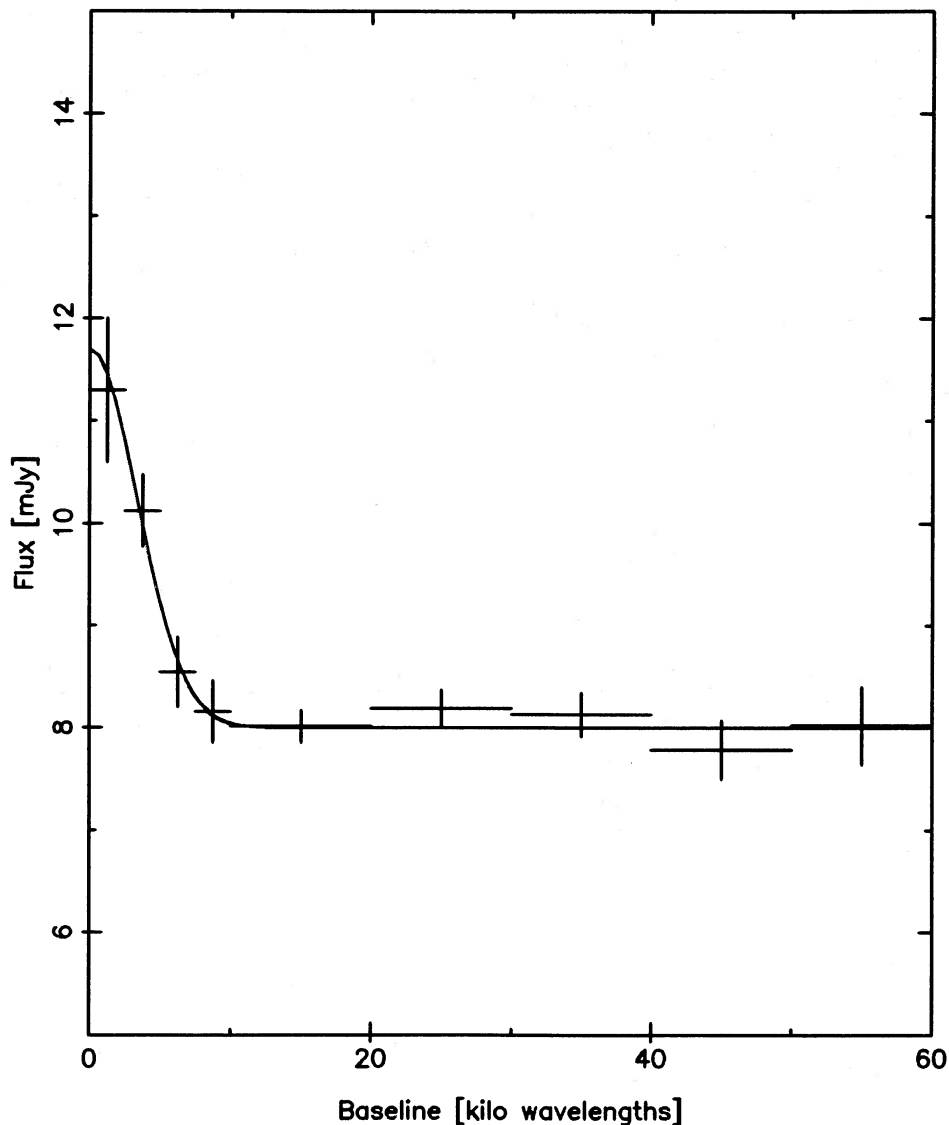


FIG. 2b

clear detection of S1 in the V map at 5 GHz; a similar figure is obtained at 15 GHz. Since these polarized emissions do not appear extended, we attribute them to the core component, whose degrees of circular polarization are 7.0% ($\pm 0.6\%$) and 7.1% ($\pm 1\%$) at 5 and 15 GHz, respectively. In addition, at 5 GHz, we have measured no linear polarization to an upper limit of 1% ($5 \times \text{rms}$).

We are confident that this result is real and not due to instrumental effects. It is true that circular polarization measurement can be difficult at the VLA. Bignell (1982) describes several hardware limitations that could affect such measurements, including beam ellipticity, beam squint, and instability of the electronics. There are, however, several reasons to consider our data as reliable.

First, internal to the observations discussed here, we note that the detections at 5 and 15 GHz are fully independent, since they were made 2 days apart with two separate detectors. At 5 GHz the V flux is constant to within 30% during the 4 hr observations. It is present in both the A/C and B/D intermediate frequencies and does not differ by more than 10%

between the two bandwidths separated by 50 MHz. The phase calibrator 1622-297 with total flux density $I = 1.88$ Jy shows no circular polarization, with $V = -0.19 \pm 0.34$ mJy, although a peak of $V = -1.20$ mJy ($V/I = -0.06\%$) is seen a few arcseconds away, possibly because of the instrumental effects mentioned by Bignell. In addition, the "companion" of S1, also very close to the phase center (but admittedly weak), does not appear on the V maps (see Fig. 1b). The internal evidence thus shows no electronic, temporal, or environmental factor affecting the circular polarization during the observation.

Second, we have observed S1 on two other occasions where instrumental polarization calibration was performed. On 1985 March 23 in a hybrid A/B configuration, snapshots of S1 were obtained for 6 minutes at each of three bands. The total and circularly polarized peak flux densities and rms noise levels (in mJy) are as follows: at 1.4 GHz, $I = 4.9 \pm 0.22$, $V = 0.12 \pm 0.23$; at 5 GHz, $I = 8.0 \pm 0.4$, $V = -0.88 \pm 0.21$; and at 15 GHz, $I = 8.3 \pm 1.0$, $V = -1.32 \pm 0.53$. The effect was thus seen at the (3-4) \times rms significance level at 5 and 15

GHz, consistent with the 1987 February data described above. On 1987 August 6 in the standard A configuration, S1 was observed for 48 minutes at the three bands. The weather conditions were poor, so the 15 GHz data were not used for polarization measurements, and phase self-calibration was needed at all bands. The flux densities (in mJy) were as follows: at 1.4 GHz, $I = 6.5 \pm 0.4$, $V = -0.08 \pm 0.09$, and at 5 GHz, $I = 7.82 \pm 0.07$, $V = -0.28 \pm 0.05$. The circular polarization at 5 GHz is again confirmed at a level of $5.5 \times$ rms, though its amplitude is significantly lower than in the 1987 February data. We conclude that circular polarization is truly present at 5 and 15 GHz at a level of 4%–7% of the total core flux; at 1.4 GHz there are only upper limits, with $3 \times$ rms values $|V/I| < 15\%$ and 4% for 1985 March and 1987 August, respectively. The circular polarization keeps the same sign whenever it is positively detected at a given frequency.

We also emphasize the high signal-to-noise ratio of the 1987 February results, reached because of the long duration of the observations, combined with the use of natural weighting to reduce the visibility data. At this low level, we cannot detect the circular polarization at 15 GHz when using the more conventional but less sensitive uniform weighting.

The radio source associated with S1 thus consists of a circularly polarized, hence magnetized core surrounded by a halo which must be thermal because it is extended. By contrast, the unresolved nature of the core has been confirmed by 1987 August observations, for which the beam was $0''.15 \times 0''.14$ at 15 GHz. The core is particularly puzzling because of our early observations of S1 did not indicate a nonthermal nature of the source. First, the variability study of Stine *et al.* (1988) shows that the total emission from S1, dominated by the emission of the core, is stable. It showed no significant variations ($< 10\%$ – 20%) at 1.4 and 5 GHz over several years, in contrast to the continuous variability exhibited by the flaring ρ Oph radio stars such as DoAr 21. The 5 GHz flux appeared also constant, to within 10%, when dividing the 4 hr 1987 observations into 30 minute scans. Second, the radio spectrum of the core given by our 1985 March observations in A/B configuration¹ showed $\alpha(1.5 \text{ GHz}, 4.9 \text{ GHz}) = 0.4 \pm 0.1$, and $\alpha(4.9 \text{ GHz}, 15 \text{ GHz}) = 0.0 \pm 0.1$ (see Fig. 4), where $S_\nu \propto \nu^\alpha$. A 115 GHz continuum upper limit of 70 mJy ($\sim 2 \times$ rms) was obtained from quick-look observation with the Owens Valley interferometer (A. I. Sargent and L. G. Munday 1986, private communication). This 1.5–15 GHz radio spectrum is flatter than many nonthermal spectra; it is perfectly consistent with our 1987 flux densities for the core that give $\alpha(5, 15) = 0.0 \pm 0.1$.

III. PROPERTIES AT OTHER WAVELENGTHS

a) Underlying Star

S1 is among the brightest stars of the ρ Ophiuchi cloud in the red and near-infrared bands ($R = 14.2$, $K = 6.3$) but is rather faint in the blue ($B = 19.7$, $V = 19.0$) because of strong interstellar reddening (Elias 1978; Chini 1981). Its broad-band energy distribution from B to N ($12 \mu\text{m}$) does not show any near-infrared excess, and is consistent with the blackbody emission of a photosphere with an effective temperature T_{eff} of

¹ Given the size of $\geq 10''$ estimated above for the halo, the VLA in A/B configuration is only sensitive to the core component. S1 was actually unresolved (on the maps as well as on the visibility curves) at 5 and 15 GHz in our 1985 March observations. At 1.5 GHz we estimated the core flux density after clipping all baselines shorter than $10 \text{ k}\lambda$ (see Fig. 2) because of a marginal contamination by the halo.

order 16,000 K, radius $r_* \sim 3 \times 10^{11}$ cm, and visual extinction $A_v \sim 12$ (from the data of Lada and Wilking 1984). Therefore its bolometric luminosity L_{bol} is on the order of $1100 L_\odot$, which indicates that S1 must be a B3–B5 star close to, or on, the main sequence. Such an early type is confirmed by the observed far-infrared luminosity and by the radio data (see below). Unfortunately, as a result of high extinction, a reliable optical spectral type for the star is not available. As part of a spectroscopic study of optical counterparts to X-ray sources of the cloud (Bouvier and Appenzeller 1987), J. Bouvier has obtained a low-resolution optical spectrum of S1, which allows the spectral type to be B, A, or F. This spectrum does not show any emission lines and, in particular, shows $H\alpha$ weakly in absorption.

S1 is also associated with the *Einstein* X-ray source ROX-14 from the survey of MKFG. Unfortunately, owing to the low count rate (minimum: 5 ± 2 , maximum 17 ± 3 , in units of 10^{-3} IPC counts s^{-1}), no spectrum can be reliably derived. Using a visual extinction $A_v \sim 10$ leads to an absorption column density of $N_{\text{H}} = (2-3) \times 10^{22} \text{ cm}^{-2}$ taking $A_v/E_{B-V} = 3$. The corresponding intrinsic X-ray luminosity, assuming a thermal bremsstrahlung spectrum with $kT \sim 1$ keV typical of ROX sources (MKFG), is $L_x = 5 \times 10^{30} - 3 \times 10^{32} \text{ ergs s}^{-1}$, making S1 an X-ray source ~ 10 – 600 times brighter than a typical main-sequence B star for which $L_x/L_{\text{bol}} \sim 10^{-7}$ (Pallavicini *et al.* 1981). This X-ray luminosity corresponds to a volume emission measure $\text{EM}_x \sim 10^{54} - 6 \times 10^{55} \text{ cm}^{-3}$ (Gaetz and Salpeter 1983).

b) Circumstellar Environment

S1 has been known as the brightest far-infrared source of the cloud (observed luminosity $\sim 400 L_\odot$ between 40 and $350 \mu\text{m}$) since the observations of Fazio *et al.* (1976). The corresponding *IRAS* point source (16235–2416), nominally located $\sim 20''$ away from the star while the *IRAS* beam is $\sim 1'$, has an energy distribution steeply rising at longer wavelengths, giving a strong flux ($4650 \pm 500 \text{ Jy}$) at $100 \mu\text{m}$ and an integrated luminosity of $170 L_\odot$ between 10 and $100 \mu\text{m}$ (Mozurkewich, Schwartz, and Smith 1986). Such a distribution is similar to that of compact H II regions detected by *IRAS* (Chini *et al.* 1986). The 35– $175 \mu\text{m}$ mappings of Harvey, Campbell, and Hoffman (1979, hereafter HCH) with a $\sim 40''$ beam show that the far-infrared source is actually extended, with a peak emission $\sim 50''$ west of S1 and a temperature increasing toward the star. This far-infrared emission appears to be correlated with the molecular distribution (mapped using 2 mm H_2CO emission) which shows a steep density gradient toward the ρ Oph A core. This core ($n \sim 3 \times 10^5 \text{ cm}^{-3}$) is located 1.9 (i.e., ~ 0.1 pc) west of S1, where the average density is $\sim 10^5 \text{ cm}^{-3}$ (Loren, Sandqvist, and Wooten 1983). It is likely that S1 is the heating source of the region and has created a low-density cavity in the dust and gas distributions around it (HCH). If this is the case, the bolometric luminosity of S1 has to be significantly larger than $400 L_\odot$ because there is insufficient dust to absorb the stellar flux on the eastern side (HCH). On a smaller scale, the preliminary detection of CO $J = 1-0$ emission by the OVRO interferometer on the line of sight of S1 suggests the existence of a large concentration/annulus/ring of molecular gas around the star, of angular diameter $\sim 10''$ – $30''$.

IV. INTERPRETATION OF THE S1 RADIO HALO

The visibility curves shown on Figure 2 yield nominal values of $\sim 10''$ for the half-power angular radius of the radio halo. This visibility analysis assumes spherical symmetry, although

the map of Figure 1 shows that asymmetric extended wings exist. This procedure provides the best estimate for the flux density of the core, but it should not be trusted for estimating the flux and size of the halo, because the information at very short baselines (less than ~ 1 k λ at 6 cm, corresponding to sizes larger than $\sim 45''$) is almost absent for the VLA in C/D configuration. From the map of Figure 1, we estimate that the halo has an extent of up to $\sim 30''$ from the central source (i.e., a linear radius greater than 6×10^{16} cm). (This does not include the "companion" $\sim 45''$ to the southeast.) This figure is consistent with the CO data from OVRO (see § IIIb), if interpreted in terms of a cavity. The large size and weak flux (giving a low brightness temperature very much less than 10^4 K), together with the flat spectrum [$\alpha(5 \text{ GHz}, 15 \text{ GHz}) \sim -0.1 \pm 0.3$] of the halo, imply free-free emission from an optically thin H II region as originally proposed by Brown and Zuckerman (1975) and Falgarone and Gilmore (1981) for the entire radio source. For a measured value of ~ 4 mJy at 5 GHz and an assumed temperature $T_i = 10^4$ K, the volume emission measure is $EM_{\text{H II}} \sim 3.5 \times 10^{55} \text{ cm}^{-3}$, requiring $N_{\text{Ly}\alpha} \sim 9 \times 10^{42} \text{ s}^{-1}$ Lyman continuum photons. This corresponds to photoionization by a \sim B3.5 ZAMS star with $T_{\text{eff}} = 17,000$ K (Thompson 1984). This temperature is fully consistent with that derived from the near-IR data discussed in § IIIa). The anisotropic interstellar distribution that may surround S1 (§ IIIb) would induce a "champagne"-like H II region, with a rapidly decreasing flux per unit area away from the molecular core (Yorke, Tenorio-Tagle, and Bodenheimer 1983). Hence, we cannot strictly rule out a larger H II region toward the northeast, which would imply a larger flux and an earlier spectral type for S1, reaching ~ 30 mJy for $T_{\text{eff}} = 19,000$ K (type \sim B2.5). We note that this optically thin halo allows the underlying radio emission from the core to escape and does not affect its brightness temperature significantly.

This analysis also allows a derivation of an age estimate for S1. Even in the "champagne" description of the evolution of an H II region, the age is very nearly given by its radius r_i in the densest regions (density n_0). Therefore, applying standard formulae (e.g., Spitzer 1978), and verifying *a posteriori* that r_i is very much greater than the initial Strömgren sphere radius, the age of S1 is

$$t_*(\text{yr}) = 10^3 (C_{\text{II}}/10 \text{ km s}^{-1})^{-1} [r_i(t)/10^{16} \text{ cm}]^{7/4} \\ \times (N_{\text{Ly}\alpha}/10^{43} \text{ s}^{-1})^{-1/4} (n_0/10^5 \text{ cm}^{-3})^{1/2}, \quad (1)$$

where C_{II} is the sound velocity. For r_i corresponding to an angular radius $\theta_i = 10''$ as estimated from the visibility data, one has $t_* \sim 5 \times 10^3$ yr. Assuming that $N_{\text{Ly}\alpha}$ has remained constant for $t < t_*$, this is actually a lower limit to the real age, since we cannot exclude the presence of an undetected weak emission farther out.

V. IMPLICATIONS OF THE OBSERVATIONS OF THE S1 RADIO CORE

a) S1 as a Magnetized B Star

Since we have repeatedly found circular polarization, we have direct and compelling evidence that the radio emission comes from a magnetized region. The broad and flat spectrum, steady flux, and modest circular polarization, as well as the observed brightness temperature (see below) of the S1 radio core, is compatible with a noncoherent mechanism. Synchrotron radiation from ultrarelativistic electrons can be discarded because the observed degree of circular polarization ($\lesssim 7\%$) implies that the emitting electrons have energies not in excess

of a few tens of MeV, even in the most favorable case of an optically thin homogeneous source (Legg and Westfold 1968). If the radio emission comes from mildly relativistic electrons, a magnetic field strength of at least 1–10 G is required in the emitting region, and the effective electron temperature $T_{\text{eff},e}$ is $\lesssim 10^{10}$ K. The brightness temperature T_b is necessarily much smaller than $T_{\text{eff},e}$ because the flat spectrum implies that most of the flux comes from optically thin regions. Since for the S1 core T_b is related to the source size l by $T_b(5 \text{ GHz}) = (3 \times 10^{10} \text{ K})(l/r_*)^{-2}$, the size of the magnetized emitting region appears quite large at the outset, on the order of a few stellar radii.

The fact that we observe a net circular polarization from this large region suggests that the orientation of the magnetic field is not random but is organized within the whole source, in contrast, for instance, with the tangled fields associated with the numerous active regions on the Sun. In this respect, it is significant that the few (nonsolar) astrophysical radio sources for which incoherent emission with substantial ($> 5\%$) net circular polarization has reliably been detected, namely, Jupiter and RS CVn binary systems, are observed or are thought to be surrounded by large and ordered magnetospheres (de Pater and Jaffe 1984; Mutel *et al.* 1987). Furthermore, we always detected the same helicity whenever we could measure a circular polarization at a given frequency. This situation is again reminiscent of RS CVn stars (Mutel *et al.* 1987), and also calls for S1 having a persistent and ordered magnetic structure.

However, in contrast with RS CVn systems, the radio emission from S1 displays weak or absent variability between observations randomly separated in time, on time scales from hours to years. This has two consequences: (1) flare mechanisms, known to operate in the case of RS CVn systems and the PMS star DoAr 21, are excluded; (2) the magnetic structure, as a whole, must be permanent (in contrast, for example, with the expanding loops suggested by Mutel *et al.* 1985 for RS CVn stars) and have a high degree of axial symmetry, since the radio flux apparently depends very little on the phase of a presumably rotating star.

The simplest conceivable configuration fulfilling the above requirements in a symmetric magnetosphere consisting in dipolar field lines surrounding the star. We will assume such a configuration in what follows. (The dipole axis may be tilted, or offset, with respect to the rotation axis, but we have too few data to take explicitly possible geometric effects into account.)

On the other hand, § IV has shown that, based on IR and radio data, S1 is very likely an early B star. S1 appears therefore reminiscent of the magnetic, chemically peculiar Bp stars characterized by strong helium lines and surface magnetic fields of a few kilogauss. These magnetic stars have recently been shown to make up a new class of radio stars (Drake *et al.* 1985, 1987). Like S1, all these objects are very likely "surface nonthermal emitters" as opposed to "wind nonthermal emitters," using the classification scheme of Abbott, Bieging, and Churchwell (1985) for early-type radio stars. The best-documented radio-emitting Bp star is the helium-rich B2 V star σ Ori E, which has been thoroughly observed in the optical and infrared domains. This star is a rapid oblique rotator ($P = 1.2$ days, $\theta = 90^\circ$) for which Landstreet and Borra (1978) have measured a mean longitudinal magnetic field consistent with a dipole of polar value $B_* \sim 10$ kG. Its radio properties ($L_{5 \text{ GHz}} \sim 6 \times 10^{17} \text{ ergs s}^{-1} \text{ Hz}^{-1}$, flat spectrum in the ~ 1 –15 GHz range, no flarelike variability; Drake *et al.* 1987) are very similar to those of S1 (for which $L_{5 \text{ GHz}} = 2.5 \times 10^{17} \text{ ergs s}^{-1} \text{ Hz}^{-1}$), though no circular polarization has

been detected to date (our estimate of the upper limit is $\sim 5\%$). Furthermore, σ Ori E has an X-ray luminosity of the same order as that estimated above for S1 (Drake *et al.* 1987), and, more generally, there is some indication that chemically peculiar magnetic stars emit X-rays at somewhat higher levels than normal B–A stars (Golub *et al.* 1983). If we add the fact that, as for S1, no significant near-infrared excess (at least of the kind observed from most young stellar objects; e.g., Lada and Wilking 1984) is observed from early-type magnetic stars (Odell and Lebofsky 1984), we find that there is ample evidence to justify considering the possibility that S1 is itself a magnetic B star.

b) Magnetospheric Configuration

The above arguments have thus led us to a hypothetical, but persuasive, picture of S1 as a rotating B star surrounded by a large magnetosphere. In addition, by analogy with chemically peculiar Bp stars, S1 probably features a moderate stellar wind. Indeed, the current interpretation of the overabundance of helium in the Bp–Ap stars (Michaud *et al.* 1987) is that, because of the strong magnetic field, mass loss is strongly inhibited along the equator, resulting in a slow diffusion of (mainly) hydrogen and helium across the field lines. In turn, the diffusion processes act selectively on the atomic species, resulting in a relative accumulation of He above the photosphere in the equatorial regions. Using a selective wind model, Michaud *et al.* have computed that the helium enrichment takes place over a few million years if the mass-loss rate in the equatorial regions is $\dot{M}_E \sim 10^{-13}$ to $10^{-12} M_\odot \text{ yr}^{-1}$. The wind is here actually a very slow breeze, since the velocity is governed by diffusion perpendicular to the field lines (see discussion in Michaud 1986). In contrast, in the polar regions covering a solid angle Ω_p , the outflow is essentially unimpeded and the standard mass-loss rate and velocity for radiatively driven winds in normal early B stars (e.g., Lamers 1981) must apply, i.e., $\dot{M}_p \sim (\Omega_p/4\pi) \times 10^{-9} M_\odot \text{ yr}^{-1}$, $V_\infty \sim 500\text{--}1000 \text{ km s}^{-1}$. Observationally, this mass-loss rate dominates \dot{M}_E , and the mass loss rate \dot{M} determined from UV spectra is $\sim \dot{M}_p$; for σ Ori E the values measured from *IUE* observations (Drake *et al.* 1987) are $\dot{M} < 10^{-9} M_\odot \text{ yr}^{-1}$ and $V_\infty = 600 \text{ km s}^{-1}$.

There is therefore a strong interplay between the material outflowing from the star and the magnetic field, which shapes the magnetospheric configuration as sketched in Figure 3a. Qualitatively, in the inner magnetosphere (i.e., close to the surface of the star) the magnetic pressure dominates, and the configuration is that of a (possibly tilted) dipole: $B \propto r^{-3}$. As r increases along the equator, the magnetic pressure goes down ($\propto r^{-6}$) but the gas pressure goes up, for two reasons: because of an increasing centrifugal force ($\propto r$) and because of an increasing density as the flow is channeled between field lines connected to higher and higher latitudes on the stellar surface, where the mass-loss rate is higher owing to the increasing role of radiative acceleration. Therefore, at some point r_1 which defines the frontier between the “inner” and the “middle” magnetospheres, the gas pressure begins to distort the field lines from their force-free (dipolar) configuration. Their exact structure is difficult to know, but they must break open at some point r_2 in the equatorial plane, which therefore marks the end of the “closed” magnetosphere. In the “outer” magnetosphere, defined by $r > r_2$, the wind dominates the magnetic field and the field lines are open. Because of rotation, the radial dependence of the magnetic field strength scales as r^{-n} with n between 1 and 2 depending on the extent to which corotation is

enforced and the corresponding importance of the toroidal component of the field. In particular, $n = 1$ is expected in the spiral field configuration of a stellar wind far from the surface of a nearly parallel rotator (Weber and Davis 1967), and is actually observed in the case of the solar wind (Burlaga *et al.* 1984). For $r_1 < r < r_2$, the magnetic and gas pressures are similar, and n depends on the exact configuration, which may be complicated, as the example of the Jovian magnetosphere shows (Connerney, Acuña, and Ness 1981; Behannon, Burlaga, and Ness 1981).

The scale of the magnetosphere can be roughly fixed by assuming a dipolar magnetic field all the way to the Alfvénic surface, beyond which the wind flows freely (e.g., Mestel and Spruit 1987; Shore 1987). A first estimate of the Alfvén radius r_A is then formally determined by matching the ram pressure of the wind ρV_∞^2 ($\propto r^{-2}$) corresponding to a spherical mass-loss rate \dot{M} (assuming it has reached its terminal velocity V_∞) and the dipolar magnetic pressure $B^2/8\pi$. Specifically, this gives

$$r_A/r_* = (B_*^2 r_*^2 / 2\dot{M}V_\infty)^{1/4}, \quad (2a)$$

or

$$r_A/r_* \sim 50(B_*/10^4 \text{ G})^{1/2} (\dot{M}/10^{-10} M_\odot \text{ yr}^{-1})^{-1/4} \\ \times (V_\infty/1000 \text{ km s}^{-1})^{-1/4} (r_*/3 \times 10^{11} \text{ cm})^{1/2}. \quad (2b)$$

Another estimate of r_A is given by the point at which the corotation of the wind can no longer be enforced by the dipolar surface magnetic field:

$$r_A/r_* = (B_*^2 V_\infty / \dot{M} \omega^2)^{1/6}, \quad (3a)$$

where $\omega = 2\pi/P$ is the stellar angular velocity, or

$$r_A/r_* \sim 26(B_*/10^4 \text{ G})^{1/3} (\dot{M}/10^{-10} M_\odot \text{ yr}^{-1})^{-1/6} \\ \times (V_\infty/1000 \text{ km s}^{-1})^{1/6} (P/1 \text{ day})^{1/3}. \quad (3b)$$

The Alfvénic zone thus corresponds to a range of radii, $r_1 \lesssim r_A \lesssim r_2$, which defines the middle magnetosphere. In practice, the above estimates lead to comparable figures, and the exact meaning of r_A is not very important.

Havnes and Goertz (1984, hereafter HG) have addressed more quantitatively the interplay between the stellar wind and a dipolar magnetic field along the equator of a parallel rapid rotator. The picture which emerges from their study consists of a dense inner region with a chromospheric temperature ($n_{\text{ch}} \sim 10^{12} \text{ cm}^{-3}$ at the equator, $T_{\text{ch}} = 8250 \text{ K}$) extending from ~ 3 to $\sim 10 r_*$, surrounded by a toroidal stellar corona ($n_c \sim 10^8 \text{ cm}^{-3}$, $T_c \sim 10^7 \text{ K}$) extending to $\sim 30 r_*$. They suggest that instabilities and magnetic reconnection occur in the middle magnetosphere, and that the corresponding release of magnetic energy (replenished by the stellar rotational energy) heats the outer regions of the closed magnetosphere (i.e., at $r \sim r_A$) up to soft X-ray temperatures, leading to the existence of the corona. The temperature depends strongly on the mass-loss rate \dot{M}_A at $r \sim r_A$, and reaches $\sim 10^7 \text{ K}$ for $\dot{M}_A \sim 10^{-10} M_\odot \text{ yr}^{-1}$. Since $r_A \gtrsim 10 r_*$, which, in a dipolar configuration, corresponds to high stellar latitudes ($\gtrsim 70^\circ$ above the equator, i.e., $\Omega_p/4\pi \lesssim 0.1$; Drake *et al.* 1987, Shore 1987), this value of \dot{M}_A is quite compatible with the fact that it is $\sim \dot{M}_p$ and $(10^2\text{--}10^3) \dot{M}_E$.

Available optical observations of S1 are not sufficient, at present, to confirm the presence of a dense chromosphere-like region around the star. However, in the case of σ Ori E, such an inner magnetosphere is directly observed in the form of

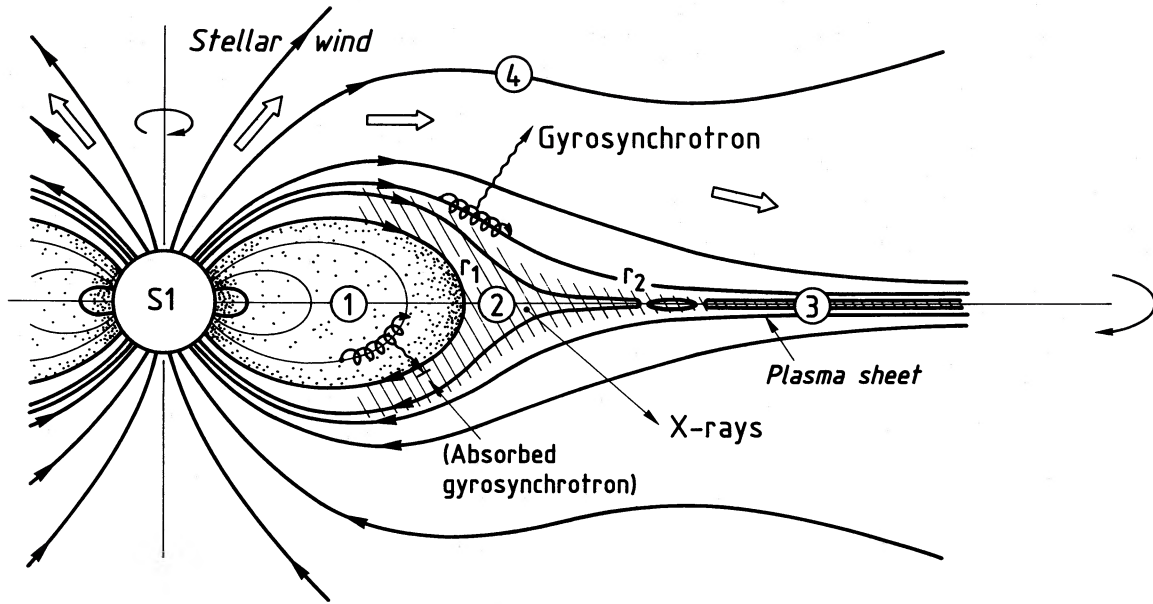


FIG. 3a

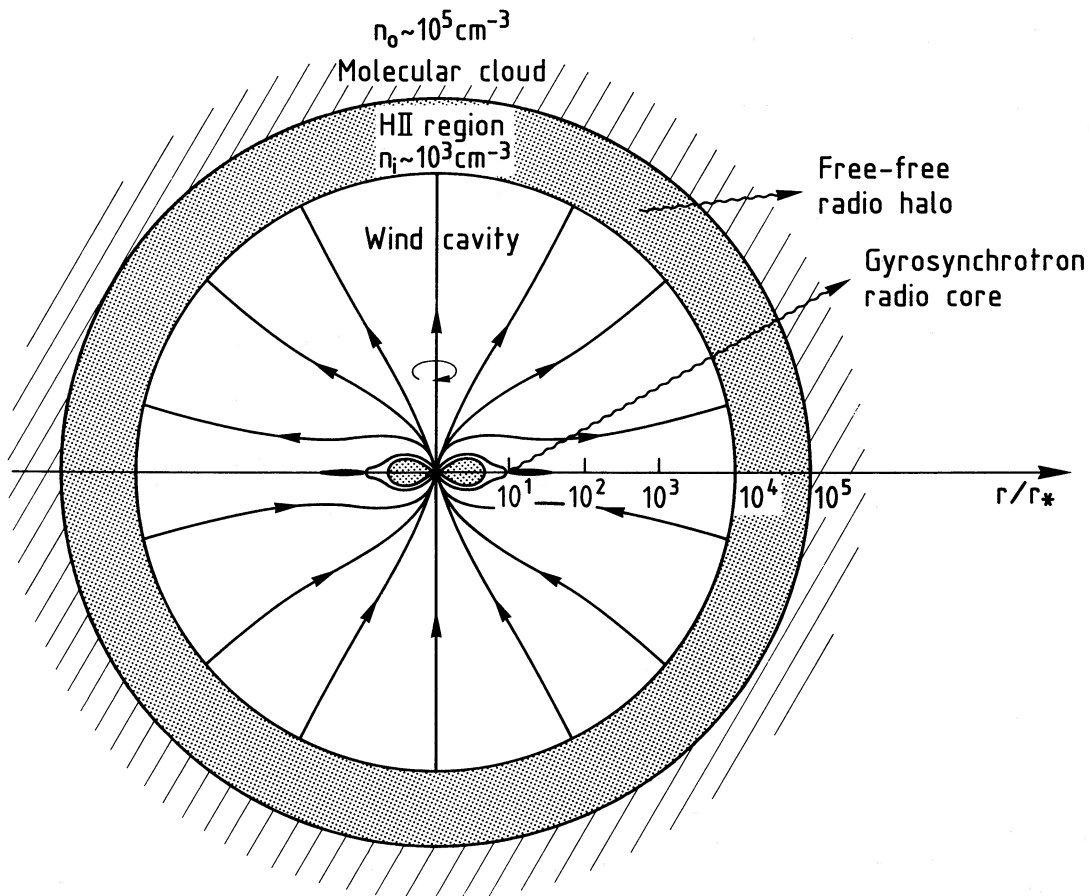


FIG. 3b

FIG. 3.—(a) Sketch of the magnetosphere surrounding S1 emphasizing the various regions. Out to r_1 , the inner magnetosphere (1) is closed and filled by an equatorial diffusive wind ($\sim 10^{-13}$ to $10^{-12} M_{\odot} \text{ yr}^{-1}$). It is a dense chromosphere-like region which is opaque to radio emission. The middle magnetosphere (2) is heated to coronal temperatures and emits X-rays; this region is still partly opaque in the radio. The stellar wind opens the magnetic field lines beyond r_2 , and shapes the outer magnetosphere (3) in the form of a plasma sheet where MeV electrons are continuously accelerated. The energetic electrons diffuse from their acceleration site and eventually feed the whole magnetosphere. The last important region (4) is dominated by the wind ($\sim 10^{-10} M_{\odot} \text{ yr}^{-1}$) that flows almost unimpeded from the poles of the star. Regions (3) and (4) emit the bulk of the observed emission via the gyrosynchrotron mechanism. (b) Large-scale picture of the environment of S1 showing the relative sizes of the core-halo structure of the radio source, in a logarithmic scale.

H α -emitting corotating clouds (see Groote and Hunger 1982; Walborn and Hesser 1976).

On the other hand, the corona predicted by HG for rotating magnetic stars provide a natural explanation for the X-ray emission of S1: a density $n_c \sim 10^8 \text{ cm}^{-3}$ and radius $r_c \sim r_A \sim 10 r_*$ give an emission measure $\text{EM}_c \sim 2\pi n_c^2 r_c^3 \sim 2 \times 10^{54} \text{ cm}^{-3}$, in fair agreement with the observed EM_x (see § IIIa).

c) Influence of the Stellar Wind on the Surrounding Medium

For $r \gg r_A$, the wind is essentially radial, and creates a cavity inside the H II region excited by S1. The mass loss, coming mostly from the polar regions, is $\dot{M} \sim \dot{M}_p$. At the boundary of the cavity, the wind energy is efficiently dissipated over a short distance (Dorland and Montmerle 1987), and the radius of the wind cavity r_{wc} is obtained simply by equating the pressures of the wind and the ionized gas of the H II region (density $n_i \lesssim 10^3 \text{ cm}^{-3}$ from the radio halo observations [see § IV]; $T_i \sim 10^4 \text{ K}$):

$$r_{wc} = 6 \times 10^{15} \text{ cm} \times [(\dot{M}/10^{-10} M_\odot \text{ yr}^{-1})(V_\infty/1000 \text{ km s}^{-1})]^{1/2} \times [(n_i/10^3 \text{ cm}^{-3})(T_i/10^4 \text{ K})]^{-1/2}. \quad (4)$$

Given that the outer radius of the H II region in the dense part of the molecular cloud is $r_i \sim 3 \times 10^{16} \text{ cm}$, and that the terminal wind velocity is $V_\infty \sim 500\text{--}1000 \text{ km s}^{-1}$, one verifies that $r_{wc} \ll r_i^3$, i.e., that the presence of a wind cavity does not affect the interpretation of the radio halo around S1.

Figure 3b synthesizes all the characteristic sizes relevant to the interpretation of the core-halo structure of the S1 radio source: in units of the stellar radius r_* , the typical sizes in round numbers are $r_A \sim 10$, $r_{wc} \sim 10^4$, $r_i \sim 10^5$.

VI. QUANTITATIVE INTERPRETATION OF THE CORE EMISSION

a) Location of the Emitting Region

In the above magnetospheric configuration (Fig. 3a) the radio emission can only arise in the corona (i.e., $r \gtrsim r_c$) or farther out, in the middle and/or outer magnetosphere of S1. This is because plasma cutoff and free-free absorption prevent the escape of radio waves from the dense chromosphere-like region; its free-free optical depth is $\tau_{ch} \sim 3 \times 10^8$ at 15 GHz using a density $n_{ch} \sim 10^{12} \text{ cm}^{-3}$, size $l_{ch} \sim 3 r_*$, and temperature $T_{ch} \sim 10^4 \text{ K}$. For this reason, we do not concur with the radiation belt model proposed by Drake *et al.* (1987) to explain the radio emission of Bp stars. (In this model, the emission comes from optically thick gyrosynchrotron by mildly relativistic electrons trapped in the inner magnetosphere of these stars, i.e., $2 < r/r_* < 10$.)

On the other hand, radio emission can escape from the coronal region because the overlying stellar wind, which flows out from the poles and eventually surrounds the whole magnetosphere (see Fig. 3b), remains optically thin. Indeed, the free-free optical depth of an ionized wind of temperature T_w , from the observer to the base of the corona, is (André 1987; see also Panagia and Felli 1975):

$$\tau_w \sim 10^{-3} (\dot{M}/10^{-10} M_\odot \text{ yr}^{-1})^2 (V_\infty/1000 \text{ km s}^{-1})^{-2} \times (r_c/3 \times 10^{12} \text{ cm})^{-3} (v/5 \text{ GHz})^{-2.1} (T_w/10^4 \text{ K})^{-1.35}. \quad (5)$$

b) Radio Emission from a Thermal Hot Plasma?

Because the radio emission of the core is not variable, it is tempting to interpret it first as coming from a magnetized

plasma in thermal equilibrium. Furthermore, in this case, X-ray and radio-emitting regions could be related in a straightforward manner. In this case, there are two possible emission mechanisms, free-free and gyroresonance emission, which will be discussed in turn.

i) Free-Free Emission

This mechanism must be considered, since it can lead to a circularly polarized emission when arising in a magnetized plasma. This is because the preferential emission and absorption of the extraordinary mode result in a net polarization fraction $\sim 2(v_B/v) \cos \phi$, where v_B is the gyrofrequency and ϕ is the angle between the magnetic field and the line of sight (Dulk 1985). But it is easily seen that such a free-free emission model for the S1 core is inconsistent with the X-ray data. For $T_c \sim 10^7 \text{ K}$ and $\text{EM}_x < 6 \times 10^{55} \text{ cm}^{-3}$ (see § IIIa), the expected radio flux density at 5 GHz is at most $\sim 0.5 \text{ mJy}$ (optically thin case).

Furthermore, one cannot resort to some other thermal plasma at a different temperature from the one detected by the *Einstein Observatory*. On the one hand, the emission measure from a higher temperature plasma is severely constrained by hard X-ray observations with the *Tenma* satellite ($\text{EM}_x < 10^{55} \text{ cm}^{-3}$ for $T_c \sim 10^8 \text{ K}$; Koyama 1987), and this cannot account for more than $\sim 0.05 \text{ mJy}$ at 5 GHz. On the other hand, if the temperature is lower ($T = 10^6 \text{ K}$), an unrealistically strong magnetic field ($B \sim 500 \text{ G}$) is required in a large region ($r \sim 30 r_*$) to explain the observed 15 GHz flux and the degree of circular polarization. No reasonable mass loss can severely distort such a strong magnetic field from its original dipolar geometry, implying a $\sim r^{-3}$ dependence throughout. The field at the stellar surface would then be $B_* > 10^7 \text{ G}$, which is unreasonably high, ~ 3 orders of magnitude above the typical values detected on Bp stars.

ii) Gyroresonance Emission

Gyroresonance emission from a hot ($T_c \sim 10^7 \text{ K}$) plasma has to be considered next because it is the favored mechanism for solar active regions at frequencies above 5 GHz (Alissandrakis, Kundu, and Lantos 1980). Also, it is often invoked to explain the quiescent microwave emission from red dwarf stars (e.g., Gary 1985), and has even been suggested for early-type stars (Underhill 1984).

If such a process applies to S1, the magnetic field is constrained to be $B \sim 1000 \text{ G}$, $\sim 300 \text{ G}$, and $\sim 100 \text{ G}$ in the emitting regions at 15, 5, and 1.4 GHz, respectively. This is because gyroresonance emission is concentrated at low harmonics, with emission and absorption coefficients strongly dependent on the magnetic field (Dulk 1985). At each frequency ν , the emission sharply decreases outside the $\tau_\nu \sim 1$ surface of radius $r_1(\nu)$, so that the flux density is that of an effective blackbody:

$$F_\nu \sim \left(\frac{2kT_c \nu^2}{c^2} \right) \pi \left[\frac{r_1(\nu)}{d} \right]^2 = 0.1 \text{ mJy} \left(\frac{\nu}{5 \text{ GHz}} \right)^2 \left(\frac{T_c}{10^7 \text{ K}} \right) \left(\frac{r_1}{10^{12} \text{ cm}} \right)^2 \left(\frac{d}{160 \text{ pc}} \right)^{-2}, \quad (6)$$

assuming a source circular in shape. If $T_c \sim 10^7 \text{ K}$, this gives the sizes of emitting regions: $r_1(15 \text{ GHz}) \sim 3 \times 10^{12} \text{ cm}$, $r_1(5 \text{ GHz}) \sim 9 \times 10^{12} \text{ cm}$, and $r_1(1.4 \text{ GHz}) \sim 2.5 \times 10^{13} \text{ cm}$. We are thus led to a strong magnetic field (1000 G at $10 r_*$) varying roughly as r^{-1} between ~ 10 and $\sim 80 r_*$. This radial

dependence does not represent a potential configuration, which is consistent with the fact that the whole emitting region lies in the outer magnetosphere ($r > r_A$; see § Vb). But the field strengths derived above are far too high to permeate a region where the gas pressure dominates the magnetic pressure. A huge mass-loss rate (at least $8 \times 10^{-4} M_\odot \text{ yr}^{-1}$ if $V_\infty = 1000 \text{ km s}^{-1}$) is necessary to get $r_A = 10 r_*$ if $B(r_A) = 1000 \text{ G}$. Such a dense ionized wind is excluded, since it would be an enormous free-free emitter, producing radio and X-ray fluxes orders of magnitude above the observations. If one assumes a hotter plasma ($T_C = 10^8 \text{ K}$), the required mass-loss rate is reduced somewhat ($\sim 8 \times 10^{-6} M_\odot \text{ yr}^{-1}$), but the implied emission measure is still largely inconsistent with both radio and hard X-ray observations.

In conclusion, radio emission from a magnetized thermal plasma is inconsistent with the observed characteristics of the S1 core. Furthermore, this conclusion is rather strong, since it is largely independent of the geometry suggested in § Vb.

c) Gyrosynchrotron Emission from Nonthermal Electrons

The only remaining radio emission mechanism is thus non-thermal gyrosynchrotron from mildly relativistic ($E \sim 1 \text{ MeV}$) electrons. Since there are no direct quantitative constraints on the magnetic field configuration and on the distribution function of the energetic electrons, we will here use explicitly the magnetospheric picture described by HG and outlined in § Vb to build a working model of the emission.

We take the emitting region to be located at about $r_C \sim 10 r_*$ from the central star and having a size of the order of r_C . Then the emission is largely optically thin (as indicated in § Va), since the actual brightness temperatures ($T_b \sim 10^7 \text{ K}$, $\sim 9 \times 10^7 \text{ K}$, and $\sim 7 \times 10^8 \text{ K}$ at 15, 5, and 1.4 GHz, respectively) are much less than the effective temperature of the emitting MeV electrons ($T_{\text{eff},e} \sim 10^{10} \text{ K}$). Also, the surface magnetic field is $B_* \sim 10^4 \text{ G}$, and the coronal magnetic field is on the order of $B_*(r_C/r_*)^{-3} \sim 10 \text{ G}$.

There is ample energy to feed the relativistic electron population, as the following approximate calculation shows. Consider the radiation from an isotropic distribution of nonthermal electrons with a power-law energy spectrum $N(E) \propto E^{-\delta}$ between E_{min} and E_{max} . Owing to the flat radio spectrum, the spectrum of the energetic electrons is probably rather flat itself ($\delta = 1-2$). For $\delta = 2$ and $E_{\text{min}} = 10 \text{ keV}$, an approximation formula from Dulk and Marsh (1982) gives a number of energetic electrons if the source is optically thin and homogeneous of about $N_{\text{tot}} \sim 10^{41}$ for $F_{5 \text{ GHz}} = 8 \text{ mJy}$. With $E_{\text{max}} = 15 \text{ MeV}$, the mean energy per radiating electron is $\langle E \rangle \sim E_{\text{min}} \ln(E_{\text{max}}/E_{\text{min}}) \sim 70 \text{ keV} \sim 10^{-7} \text{ ergs}$, and the total energy is on the order of 10^{34} ergs . Since the lifetime of these electrons against synchrotron losses is on the order of 10^6 s , this implies that their energy must be replenished at a rate $L_{\text{NT}} \sim 10^{28} \text{ ergs s}^{-1}$. For a density of the coronal thermal plasma of $\sim 10^8 \text{ cm}^{-3}$, the lifetime of energetic electrons against Coulomb collisions with thermal electrons is even shorter [$\sim 8 \times 10^3 \text{ s} (\gamma - 1) (n_C/10^8 \text{ cm}^{-3})^{-1}$; e.g., Kuipers and van der Hulst 1985], raising the energy requirement to $L_{\text{NT}} \sim 10^{30} \text{ ergs s}^{-1}$. This is still much less than the thermal X-ray luminosity of the corona, $L_X \sim 10^{31}-10^{32} \text{ ergs s}^{-1}$. Finally, we note that (internal) Faraday depolarization probably accounts for our nondetection of linear polarization, as the Faraday rotation angle of the medium exceeds 10^5 radians.

It is possible to go further and find a precise spectral fit to our observational data. An inhomogeneous model of the radio

emission was computed numerically, using the methods described in detail by Klein and Trotter (1984) and the approximate gyrosynchrotron formulae of Klein (1987). In these computations, we approximate the magnetic field by a dipole located in the center of S1, and extending out to a few $10 r_*$ from the star. In such a symmetric configuration, the observer must be situated outside the equatorial plane in order to detect a net circular polarization. In our model, we take the extreme view that the magnetosphere is seen pole-on. The density profile of thermal electrons in the corona is represented by an exponential decrease, with scale height H_C , from its value $n_{C,0}$ at the base of the corona at $10 r_*$. The temperature T_C is fixed at 10^7 K everywhere in the radio source. The energetic electrons are assumed to be homogeneously and isotropically distributed with a power law of index $\delta = 1.2$. The flux density spectrum of the radio emission is then the result of gyrosynchrotron emission from the nonthermal tail, combined with free-free absorption from the thermal X-ray plasma. Figure 4 shows a flux density spectrum which reasonably fits the observed values. This theoretical spectrum was computed with the following other parameters: $B(10 r_*) = 10 \text{ G}$, $n_{C,0} = 2.3 \times 10^8 \text{ cm}^{-3}$, $H_C = 3 r_* = 9 \times 10^{11} \text{ cm}$. The values of $n_{C,0}$ and H_C yield $\text{EM}_C = 4 \times 10^{54} \text{ cm}^{-3}$. The number density of non-thermal electrons between $E_{\text{min}} = 10 \text{ keV}$ and $E_{\text{max}} = 25 \text{ MeV}$ is $n_{\text{NT}} = 6 \text{ cm}^{-3}$. The physical parameters of the thermal plasma are in satisfactory agreement with those derived from the X-ray observations. Since a total of 2×10^{40} electrons above 10 keV is involved, which represents an energy content of $2 \times 10^{34} \text{ ergs}$, we note that the energy estimates given above for a homogeneous source are confirmed by this more detailed emission model.

In this dipolar model of the S1 radio emission, the outer boundary of the source is essentially determined by the outward decrease of the magnetic field, while the inner boundary is fixed by the free-free absorption due to the thermal component of the corona. The low-frequency source extends up to about $30 r_*$ from the center of the star, and the source size decreases with increasing frequency (cf. Klein and Chiuderi-Drago 1987). Actually, the real extent of the source is likely to be larger, since the magnetic field is expected to decrease more slowly than a perfect dipole in the emitting region (§ Vb). However, because the emission is optically thin, the dipolar approximation of the field, and the assumption that the observer is situated on the polar axis, are probably not critical as far as the flux density spectrum is concerned.

It is, however, crucial for the circular polarization. Because of the contribution from the whole stellar magnetosphere, where the magnetic field orientation and strength vary with respect to the line of sight, the observed polarization cannot be compared with the prediction of homogeneous models (e.g., Dulk 1985). The computation of circular polarization in a non-uniform magnetic field requires a detailed knowledge of the plasma-magnetic field configuration in and around the source. This is because circular polarization depends on the viewing angle, and because wave propagation may depend on the frequency (for instance, via mode coupling; see Melrose 1980). We lack this knowledge, and we therefore limit ourselves to the statement that some net circular polarization will arise from an ordered magnetosphere, as long as the observer is not situated in the plane of the magnetic equator. In addition, we note that in the case of the much better observed solar microwave bursts, the circular polarization cannot be computed either (see the discussion in Alissandrakis and Preka-Papadema 1984). As for

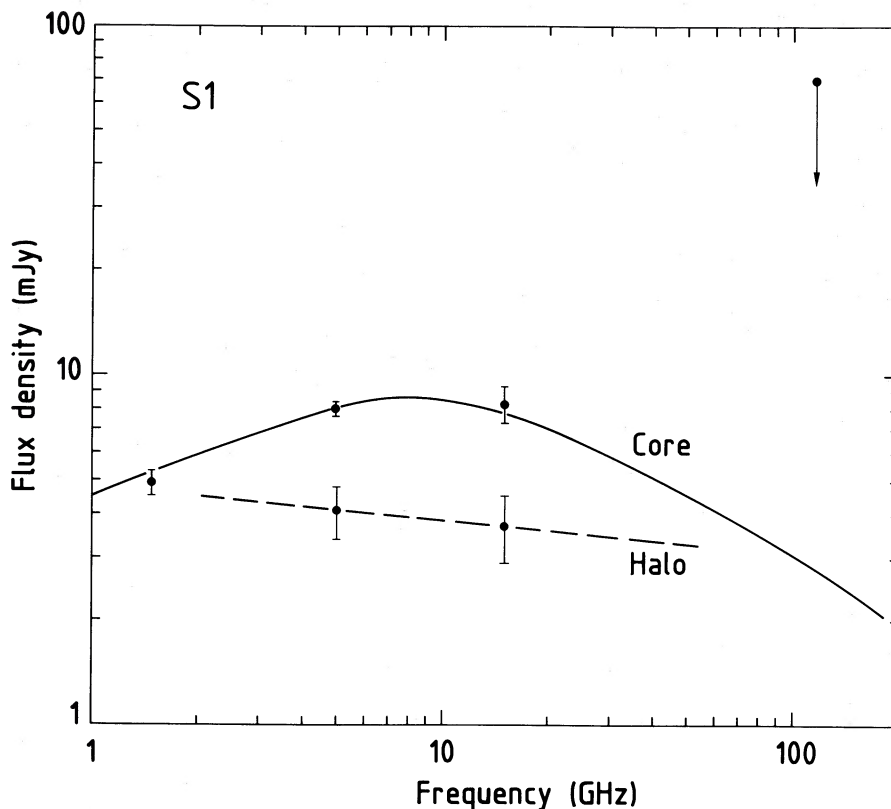


FIG. 4.—Radio spectra of the S1 core (*top*) and halo (*bottom*). The 1.5, 5, and 15 GHz points for the core are from observations performed in 1985 March while the VLA was in A/B configuration. The error bars include the calibration uncertainty. The solid curve represents a fit to the core emission using our gyrosynchrotron model. The 5 and 15 GHz points for the halo are from the visibility analysis of the present VLA C/D 1987 February observations (see § IIb). The dashed line gives the spectrum of an optically thin H II region. The upper limit at 115 GHz is from quick-look observations with the OVRO interferometer.

S1, the scanty available data certainly do not justify a more elaborate model, and any quantitative analysis of the circular polarization is thus precluded.

d) Possible Origin of the Energetic Electrons

The gyrosynchrotron interpretation described above requires a mechanism able to replenish a steady state population of \sim MeV electrons, in order to account for the steady radio emission. First, we note that the presence of high-energy particles is a typical feature of rotating magnetospheres. For instance, *in situ* measurements by the *Voyager* and *Pioneer* spacecraft have shown the ubiquity of such energetic particles, with energies of up to several tens of MeV, in the rapidly rotating Jovian magnetosphere (Schardt and Goertz 1983). Very flat energy spectra (of the kind required by the gyrosynchrotron model of § VIc) are measured for the electrons ($\delta \sim 1.5$; Baker and Van Allen 1976); such spectra are also observed in the interplanetary space (e.g., Lin 1985). Although the source of energy in planetary magnetospheres is not yet fully understood on theoretical grounds, the dynamo created by the interaction between the solar wind and these strongly magnetized bodies is certainly a key ingredient (Akosofu 1982). In the case of Jupiter, the dissipation of the rotational energy is also thought to play a central role (Goertz 1986). In our picture, S1 does possess the key properties necessary for particle acceleration: flowing ionized material and magnetic fields.

More specifically, for Jupiter, one of the proposed acceleration mechanisms is based on reconnection in the magnetotail. Since this is precisely the mechanism by which magnetic B star

coronae are heated in the view of HG, we tentatively apply this process to the magnetosphere of S1.

In the configuration discussed in § Vb, the magnetosphere is continually filled in by an equatorial diffusive wind. The density buildup leads to a rotational distortion of the initially dipolar field lines with a corresponding storage of magnetic energy. A magnetodisk is probably formed with an equatorial plasma sheet like those observed in Jupiter's magnetotail (Ness *et al.* 1979; Krimigis *et al.* 1979). In the model of § VIc, the radio-emitting region lies at the onset of this magnetotail. Now a disklike configuration is likely to have sporadic and/or steady state reconnections which release the excess magnetic energy resulting from the gas pressure at $r \sim r_A$, accelerate particles, and heat the magnetospheric plasma sheet. Once accelerated in the plasma sheet, these high-energy particles diffuse and populate the whole magnetosphere as in the Jovian case. Although the gyrosynchrotron emission due to the electrons located in the magnetotail is weakly polarized (owing to the field reversal in this region), the global radio emission can be polarized if a significant fraction of the emission arises in the parts of the outer magnetosphere where the magnetic field has a systematic component along the rotation axis (cf. Fig. 3a).

It is plausible that the dissipation of magnetic energy occurs at different places in the magnetosphere, in the form of numerous small events similar to substorms observed in planetary magnetospheres (Baker 1986). Because this process has a steady engine (the magnetically controlled stellar wind) and takes place on a very large scale (an annulus of radius exceeding $\sim 10 r_*$), the global population of energetic particles will

very likely be in a steady state. Their energy budget is more than sufficient to account for both the X-ray and the radio emissions. Indeed, the emitting regions ultimately draw their energy from the rotational energy of the star at the approximate rate (HG),

$$\begin{aligned} L_{\text{rot}} &\sim \frac{1}{2} \dot{M} (\omega r_c)^2 \\ &= 1.5 \times 10^{32} \text{ ergs s}^{-1} (\dot{M}/10^{-10} M_{\odot} \text{ yr}^{-1}) \\ &\quad \times (P/1 \text{ day})^{-2} (r_c/10 r_*)^2, \end{aligned} \quad (7)$$

which can easily be larger than L_X , itself much greater than L_{NT} .

We conclude that the magnetospheric picture of HG provides a reasonable, self-consistent interpretation of the observed X-ray and radio characteristics of S1.

VII. CONCLUSIONS

The S1 radio source consists of a nonthermal unresolved core with circular polarization, surrounded by a thermal extended halo. The halo is well interpreted as an optically thin compact H II shell which is photoionized by a young B3 star. The radio properties of the core imply the presence of a steady population of MeV electrons in an organized magnetic field of $B = 1\text{--}100$ G. Both the X-ray and the radio data would be very well explained if S1 were a rapidly rotating magnetic B star ($B_* \sim 10^4$ G). S1 is very likely similar to the radio-emitting Bp–Ap stars recently found by Drake *et al.* (1987). Contrary to nonthermal OB emitters, the radio emission does not arise from a chaotic stellar wind (White 1985), since this would imply too high a mass-loss rate as well as weak magnetic fields, ultrarelativistic electrons, and thus absence of circular polarization. The emission, which is quiescent, also differs from the highly variably radio emission observed in RS CVn systems. Our present VLA observations of S1, bringing the first detection of circular polarization from a B star, therefore confirm the suggestion by Drake *et al.* (1987) that Bp–Ap stars make up a new class of radio stars. However, we disagree with the “radiation belt” model of these authors because the inner magnetosphere of these stars is opaque to radio emission. Instead, we propose that the magnetic stars emit optically thin gyrosynchrotron radiation from their outer magnetospheres. A possible acceleration mechanism involves magnetic micro-events such as substorms in the Earth’s magnetosphere. This is supported by the current semiquantitative model of magnetospheres around these stars (HG).

However, our radio observations by themselves do not provide compelling evidence that S1 is a chemically peculiar magnetic B star. A suitable version of magnetized accretion (Uchida and Shibata 1984) may perhaps provide a viable alter-

native. On the other hand, future observations could test our interpretation. Though impeded by the strong interstellar absorption, an optical spectroscopic study should reveal a high rotational velocity ($v \sim 200$ km s $^{-1}$) of the star surface. In particular, by analogy with σ Ori E, the presence of a dense corotating chromosphere (expected in Havnes and Goertz’s configuration) should show up on an H α profile with sufficient signal-to-noise. An attempt to measure an effective stellar magnetic field by spectropolarimetry should be tried, though it is probably out of the scope of present techniques (Mathys and Stenflo 1986) owing to the faintness of the star. Also, measurements of the intensity of He lines would be invaluable to look for overabundance of helium in the S1 atmosphere. However, a negative result could simply mean that the star is too young for the enrichment already to have taken place. In the radio range, low-frequency observations may reveal emission at the gyro-frequency [$\nu_B = 0.28$ GHz ($B/100$ G)] due to auroral particles like those responsible for Jupiter’s decametric emission. Interferometric high-frequency observations (~ 100 GHz) at the ~ 1 mJy level would be decisive, but they seem beyond the reach of existing instruments.

Finally, an important question regards the status of S1 among ρ Oph radio stars and young stellar objects. On the one hand, S1 is probably associated with the only compact H II region of the whole cloud, in spite of earlier interpretations of all the stellar radio sources as being such H II regions (Brown and Zuckerman 1975; Falgarone and Gilmore 1981). On the other hand, through its magnetized core, S1 may be another representative of the ρ Oph radio stars whose main characteristic may well be the presence of extended magnetic fields (Stine *et al.* 1988), as is already the case for the flaring radio star DoAr 21. Further deep VLA observations have recently been obtained in order to detect circular polarization from other sources, and confirm this hypothesis. The results will be reported elsewhere.

We wish to thank Jérôme Bouvier for communicating optical results prior to publication and Anneila Sargent for organizing millimeter-wave observations of S1 with the Owens Valley Radio Observatory, operated by the California Institute of Technology. We also thank Edmond Roelof and Georges Michaud for enlightening discussions. Ph. A. appreciates the hospitality of the Department of Astronomy at Penn State. He is also grateful to the NRAO staff and specially to Pat Crane for assistance during the calibration of the data. The National Radio Astronomy Observatory is operated by Associated Universities, Inc., under contract with the National Science Foundation. This work was partially supported by a National Science Foundation Presidential Young Investigator Award to E. D. F.

REFERENCES

- Abbott, D. C., Biegging, J. H., and Churchwell, E. 1985, in *Radio Stars*, ed. R. M. Hjellming and D. M. Gibson (Dordrecht: Reidel), p. 219.
 Akasofu, S. I. 1982, *Ann. Rev. Astr. Ap.*, **20**, 117.
 Alissandrakis, C. E., Kundu, M. R., and Lantos, P. 1980, *Astr. Ap.*, **82**, 30.
 Alissandrakis, C. E., and Preka-Papadema, P. 1984, *Astr. Ap.*, **139**, 507.
 André, Ph. 1987, in *Protostars and Molecular Clouds*, ed. T. Montmerle and C. Bertout (Saclay: CEA/Doc), p. 143.
 André, Ph., *et al.* 1988, in preparation.
 André, Ph., Montmerle, T., and Feigelson, E. C. 1987, *A.J.*, **93**, 1182 (AMF).
 Baker, D. N. 1986, in *Magnetospheric Phenomena in Astrophysics*, ed. R. I. Epstein and W. C. Feldman (New York: AIP), p. 184.
 Baker, D. N., and Van Allen, J. A. 1976, *J. Geophys. Res.*, **81**, 617.
 Behannon, K. W., Burlaga, L. F., and Ness, N. F. 1981, *J. Geophys. Res.*, **86**, 8385.
 Bignell, R. C. 1982, in *Synthesis Mapping*, ed. A. R. Thompson and L. R. D’Addario (Green Bank: NRAO), pp. 6–8.
 Bouvier, J., and Appenzeller, I. 1988, in preparation.
 Brown, R. L., and Zuckerman, B. 1975, *Ap. J. (Letters)*, **202**, L125.

- Burlaga, L. F., Klein, L. W., Lepping, R. P., and Behannon, K. W. 1984, *J. Geophys. Res.*, **89**, 10,659.
- Chini, R. 1981, *Astr. Ap.*, **99**, 346.
- Chini, R., Kreysa, E., Mezger, P. G., and Gemund, H. P. 1986, *Astr. Ap.*, **154**, L8.
- Connerney, J. E. P., Acuña, M. H., and Ness, N. F. 1981, *J. Geophys. Res.*, **86**, 8370.
- de Pater, I., and Jaffe, W. J. 1984, *Ap. J. Suppl.*, **54**, 405.
- Dorland, H., and Montmerle, T. 1987, *Astr. Ap.*, **177**, 243.
- Drake, S. A., Abbott, D. C., Bastian, T. S., Biegging, J. H., Churchwell, E., Dulk, G., and Linsky, J. L. 1987, *Ap. J.*, **322**, 902.
- Drake, S. A., Abbott, D. C., Biegging, J. H., Churchwell, E., and Linsky, J. L. 1985, in *Radio Stars*, ed. R. M. Hjellming and D. M. Gibson (Dordrecht: Reidel), p. 247.
- Dulk, G. A. 1985, *Ann. Rev. Astr. Ap.*, **23**, 169.
- Dulk, G. A., and Marsh, K. A. 1982, *Ap. J.*, **259**, 350.
- Elias, J. H. 1978, *Ap. J.*, **224**, 453.
- Falgarone, E., and Gilmore, W. 1981, *Astr. Ap.*, **95**, 32.
- Fazio, G. G., Wright, E. L., Zeilik, M., and Low, F. J. 1976, *Ap. J. (Letters)*, **206**, L165.
- Feigelson, E. D. 1984, in *Cool Stars, Stellar Systems, and the Sun*, ed. S. L. Baliunas and L. Hartmann (Berlin: Springer), p. 27.
- . 1987, in *Protostars and Molecular Clouds*, ed. T. Montmerle and C. Bertout (Saclay: CEA/Doc), p. 123.
- Feigelson, E. D., and Montmerle, T. 1985, *Ap. J. (Letters)*, **289**, L19.
- Gaetz, T. J., and Salpeter, E. E. 1983, *Ap. J. Suppl.*, **52**, 155.
- Gary, D. E. 1985, in *Radio Stars*, ed. R. M. Hjellming and D. M. Gibson (Dordrecht: Reidel), p. 185.
- Goertz, C. K. 1986, in *Magnetospheric Phenomena in Astrophysics*, ed. R. I. Epstein and W. C. Feldman (New York: AIP), p. 208.
- Golub, L., Harnden, F. R., Jr., Maxson, C. W., Rosner, R., Vaiana, G. S., Cash, W., Jr., and Snow, T. P., Jr. 1983, *Ap. J.*, **271**, 264.
- Grasdalen, G. L., Strom, K., and Strom, S. E. 1973, *Ap. J. (Letters)*, **184**, L53.
- Groote, D., and Hunger, K. 1982, *Astr. Ap.*, **116**, 64.
- Harvey, P. M., Campbell, M. F., and Hoffmann, W. F. 1979, *Ap. J.*, **228**, 445 (HCH).
- Havnes, O., and Goertz, C. K. 1984, *Astr. Ap.*, **138**, 421.
- Klein, K. L. 1987, *Astr. Ap.*, **183**, 341.
- Klein, K. L., and Chiuderi-Drago, F. 1987, *Astr. Ap.*, **175**, 179.
- Klein, K. L., and Trotter, G. 1984, *Astr. Ap.*, **141**, 67.
- Koyama, K. 1987, *Pub. Astr. Soc. Japan*, **39**, 245.
- Krimigis, S. M., et al. 1979, *Science*, **206**, 977.
- Kuijpers, J., and van der Hulst, J. M. 1985, *Astr. Ap.*, **149**, 343.
- Lada, C. J., and Wilking, B. A. 1984, *Ap. J.*, **287**, 610.
- Lamers, H. J. G. L. M. 1981, *Ap. J.*, **245**, 593.
- Landstreet, J. D., and Borra, E. F. 1978, *Ap. J. (Letters)*, **224**, L5.
- Legg, M. P. C., and Westfold, K. C. 1968, *Ap. J.*, **154**, 499.
- Lin, R. P. 1985, *Solar Phys.*, **100**, 537.
- Loren, R. B., Sandqvist, A., Wootten, A. 1983, *Ap. J.*, **270**, 620.
- Mathys, G., and Stenflo, J. O. 1986, *Astr. Ap.*, **168**, 184.
- Melrose, D. B. 1980, in *Plasma Astrophysics*, Vol. 2 (New York: Gordon & Breach).
- Mestel, L., and Spruit, H. C. 1987, *M.N.R.A.S.*, **226**, 57.
- Michaud, G. 1986, in *Hydrogen Deficient Stars and Related Objects*, ed. K. Hunger, D. Schönberner, and N. K. Rao (Dordrecht: Reidel), p. 453.
- Michaud, G., Dupuis, J., Fontaine, G., and Montmerle, T. 1987, *Ap. J.*, **332**, 302.
- Montmerle, T., Koch-Miramond, L., Falgarone, E., and Grindlay, J. E. 1983, *Ap. J.*, **269**, 182 (MKFG).
- Mozurkewich, D., Schwartz, P. R., and Smith, H. A. 1986, *Ap. J.*, **311**, 371.
- Mutel, R. L., Lestrade, J. F., Preston, R. A., and Phillips, R. B. 1985, *Ap. J.*, **289**, 262.
- Mutel, R. L., Morris, D. H., Doiron, D. J., and Lestrade, J. F. 1987, *A.J.*, **93**, 1220.
- Ness, N. F., Acuña, M. H., Lepping, R. P., Behannon, K. W., Burlaga, L. F., and Neubauer, F. M. 1979, *Nature*, **280**, 799.
- Odell, A. P., and Lebofsky, M. 1984, *Astr. Ap.*, **140**, 468.
- Pallavicini, R., Golub, L., Rosner, R., Vaiana, G. S., Ayres, T., and Linsky, J. L. 1981, *Ap. J.*, **248**, 279.
- Panagia, N., and Felli, M. 1975, *Astr. Ap.*, **39**, 1.
- Schardt, A. W., and Goertz, C. K. 1983, in *Physics of the Jovian Magnetosphere*, ed. A. J. Dessler (Cambridge Planetary Science Series), p. 157.
- Sequist, E. R., and Taylor, A. R. 1987, *Ap. J.*, **312**, 813.
- Shore, S. N. 1987, *A.J.*, **94**, 731.
- Spitzer, L. 1978, *Physical Processes in the Interstellar Medium* (New York: Wiley), p. 254.
- Stine, P. C., Feigelson, E. D., André, Ph., and Montmerle, T. 1988, *A.J.*, in press.
- Thompson, R. I. 1984, *Ap. J.*, **283**, 165.
- Uchida, Y., and Shibata, K. 1984, *Pub. Astr. Soc. Japan*, **36**, 105.
- Underhill, A. B. 1984, *Ap. J.*, **276**, 583.
- Walborn, N. R., and Hesser, J. E. 1976, *Ap. J. (Letters)*, **205**, L87.
- Weber, E. J., and Davis, L. 1967, *Ap. J.*, **148**, 217.
- White, R. L. 1985, *Ap. J.*, **289**, 698.
- White, R. L., and Becker, R. H. 1982, *Ap. J.*, **262**, 657.
- Yorke, H. W., Tenorio-Tagle, and Bodenheimer, P. 1983, *Astr. Ap.*, **127**, 313.

PHILIPPE ANDRÉ: IRAM, Avda. Divina Pastora 7, Nucleo Central, 18012 Granada, Spain

ERIC D. FEIGELSON and PETER C. STINE: Department of Astronomy, The Pennsylvania State University, University Park, PA 16802

KARL-LUDWIG KLEIN: Observatoire de Paris, Section de Meudon, UA 324, 92195 Meudon Principal Cedex, France

THIERRY MONTMERLE: DPhG/SAP, Centre d'Etudes Nucléaires de Saclay, 91191 Gif-sur-Yvette Cedex, France